Article

Microstructure Characteristics and Wear Performance of a Carburizing Bainitic Ferrite + Martensite Si/Al-Rich Gear Steel

Yanhui Wang [1,†], Qingsong He [2,3,†], Qian Yang [1,2], Dong Xu [4], Zhinan Yang [2,*] and Fucheng Zhang [2,*]

[1] Key Laboratory of Intelligent Industrial Equipment Technology of Hebei Province, School of Mechanical and Equipment Engineering, Hebei University of Engineering, Handan 056038, China; wangyanhui@hebeu.edu.cn (Y.W.); 15033554684@163.com (Q.Y.)

[2] State Key Laboratory of Metastable Materials Science and Technology, Yanshan University, Qinhuangdao 066004, China; heqingsong@portqhd.com

[3] Qinhuangdao Port Co., Ltd. of Hebei Port Group Co., Ltd., Qinhuangdao 066002, China

[4] Technology Innovation Center for High Quality Cold Heading Steel of Hebei Province, Hebei University of Engineering, Handan 056038, China; xudong_xyz@163.com

* Correspondence: zhinanyang@ysu.edu.cn (Z.Y.); zfc@ysu.edu.cn (F.Z.)

† These authors contributed equally to this work.

Abstract: In this paper, a new low-carbon alloy gear steel is designed via Si/Al alloying. The carburizing and austempering, at a temperature slightly higher than the martensitic transformation point (Ms) of the surface and much lower than the Ms of the core, for different times, were carried out on the newly designed gear steel. After heat treatment, a series of different microstructures (superfine bainitic ferrite + retained austenite, superfine bainitic ferrite + martensite + retained austenite, and martensite + retained austenite) were obtained on the surface, whilst the low-carbon lath martensitic microstructure was obtained in the core. The microstructure of the surface was examined using optical microscopy (OM), scanning electron microscopy (SEM), and transmission electron microscopy (TEM). The phase composition was analyzed using X-ray diffraction (XRD). The hardness and wear resistance of the surface as well as the hardness distribution of carburizing layer of the samples with different microstructures were studied. The results show that the Si/Al-rich gear steel, after carburizing and austempering at 200 °C for 8 h, not only has excellent mechanical properties but also has high wear resistance, which meets the technical requirements of heavy-duty gear steel. The research work in this paper can provide a data reference for the application of carburized steel with mixed microstructures of bainitic ferrite and martensite in the design of heavy-duty gear.

Keywords: carburizing; gear steel; microstructure; wear performance; bainitic ferrite

1. Introduction

The vigorous development of the gear industry is greatly promoted by the rapid rise of today's manufacturing industry, especially the automobile industry. Gear is a precision mechanical part, which usually needs to be forged, carburized, and quenched, after cutting into teeth. Gear is easily damaged, since it will bear a variety of stresses when it works, such as impact force of variable load, contact stress, friction force, and so on, for a long time. Therefore, gear steel must have high strength, toughness, fatigue strength, and wear resistance.

At present, gear steels are mainly medium-carbon and low-carbon alloy steels. After forming, the gear parts need to be carburized and, then, undergo thermal refining (quenching + high temperature tempering). This production method has a long process time and high energy consumption. Besides, the heat treatment parameters (heating temperature, time, carburization process, etc.) have a great impact on the performance of the gear [1]. Furthermore, the deformation, which is difficult to control during heat treatment, seriously restricts the further improvement of gear quality. Therefore, it is urgent to develop environmentally friendly gear steel with better performance and lower cost.

So far, the steels used in high-speed and heavy-duty gears mainly include 20Cr2Ni4, 12Cr2Ni4, 17CrNiMo6, 18Cr2Ni4W, etc. The gear steel 20CrMnTi is widely used in China. The addition of Ti in the gear steel 20CrMnTi leads to the formation of TiN, which is of high hardness. The site of TiN is prone to a fatigue source and results in the reduced life of gear [2]. A series of carburized gear steels with high hardenability, small quenching deformation, and good mechanical properties have been manufactured in America, Japan, Germany, and other countries. The carburized gear steels in Germany are mainly Cr series, Cr–Mn series, and Cr–Mo series. The carburized gear steels in Japan are mainly Cr series and Cr–Mo series, and the carburized steels SCM882 and SNCM415 are widely used for heavy-duty gear. The Cr–Ni–Mo series of carburized gear steels are the most common ones in America, and almost all of them contain the Mo element.

In recent years, superfine bainitic steel has become one of the most popular research directions in the field of advanced steel materials because of the high strength, good plasticity, toughness, excellent wear resistance, and fatigue resistance. The main characteristics of this kind of steel are high contents of C (0.6~1.3, wt.%) and Si (1.2~3.0, wt.%), and they also contain a certain amount of Cr, Ni, Mo, Mn, and other elements. This kind of steel can perform bainite transformation at low temperatures (125~325 °C), and the nano-bainite microstructure, consisting of bainitic ferrite lath with a thickness of 20~40 nm and thin-film carbon-rich retained austenite, can be obtained [3]. The mechanical properties of nano-bainite steel are not only much better than those of the quenched and tempered steel but are, also, comparable to maraging steel. However, the cost of raw materials for nano-bainite steel is only 1/30 of that for maraging steel [4]. The ultra-high strength of nano-bainite steel is due to the nanoscale bainitic ferrite with a carbon-supersaturation state, and its excellent plasticity and toughness are derived from the thin-film carbon-rich retained austenite with high stability. Nano-bainite steel not only has better mechanical properties than all the series of bainitic steels but also has a simple production process. Nowadays, nano-bainite steel has been gradually found in many applications, such as railway tracks [5], springs [6,7], bearings [8,9], and gears [10].

Compared with conventional bainite steel, the austempering temperature of nano-bainite steel is lower, which increases the number of bainitic ferrite nucleation sites, while slowing down the speed of bainitic ferrite growth. In the early studies of nano-bainite steel, it took 2–60 days to complete the bainite transformation within the isothermal temperature range of 125–325 °C [3], which undoubtedly increases the manufacturing cost and limits its applications. In recent years, a series of significant achievements have been obtained in the exploration of accelerating bainite transformation, such as adding the alloying elements of cobalt and aluminum to the steel [11–14], making the undercooled austenite deform under different temperatures, straining before austempering [15–19], and austempering at a temperature slightly lower than the Ms point [20–24]. These methods accelerate the bainite transformation process, by shortening the incubation period or speeding up the growth rate of bainitic ferrite. However, the isothermal time required to obtain the whole nano-bainite microstructure is still the bottleneck of large-scale production for nano-bainite steel in the industry.

To shorten the production period of bainitic steel and make full use of the advantages of martensite and bainite, researchers have recently developed the bainite-martensite composite quenching process [25–29]. Studies have shown that the mixed microstructure of martensite and bainite not only accelerates the entire phase transformation process and shortens the production period, but also gives the steel high strength and toughness.

In this paper, a new low-carbon alloy gear steel is designed via Si/Al alloying. The addition of aluminum can not only accelerate the bainite transformation but also play a similar role to Si in hindering the precipitation of carbide [4,10]. This paper considers not only taking advantage of superfine bainitic ferrite in improving the performance of surface of the gear steel, but also making use of the austempering process to enhance the toughness of martensite in core. Thus, after carburizing, the austempering temperatures were selected at slightly higher than the Ms of the surface and much lower than the Ms of the core. After

carburizing and austempering, martensitic and bainitic composite microstructure gear steel with a short heat treatment period and excellent mechanical properties was prepared, which is expected to be utilized in heavy-duty gears.

2. Materials and Methods

The experimental steel was smelted in an electric furnace under vacuum condition and cast to ingot, whose chemical composition is Fe-0.20C-0.72Mn-0.74Si-1.26Ni-1.45Cr-0.34Mo-0.78Al (wt.%). Then, it was forged into steel rods with a diameter of 60 mm and annealed at 700 °C after forging. The phase-transition temperatures of the experimental steel were tested by Gleeble-3500. The test results showed that the phase transformation temperatures were Ac_1 = 762 °C, Ac_3 = 865 °C, and M_S = 365 °C, respectively. A cylinder carburized specimen with an outer diameter of 10 mm, an inner diameter of 6 mm, and a length of 70 mm was used to test the M_S temperature of the carburized surface. The specific test procedure was: with a temperature rate of 10 °C/s rising to 600 °C from room temperature, then, with a temperature rate of 1 °C/s rinsing to 900 °C, holding for 30 min, and, next, with a temperature rate of 30 °C/s dropping to room temperature. The test results showed that the M_S of the carburized surface layer was 195 °C.

The carburizing and heat treatment processes is shown in Figure 1. Firstly, the specimens were carburized in a drop-injection-controlled atmosphere full-automatic carburizing furnace, model RQ_2-25-9. The specimens were carburized at 930 °C for 10 h. The first 8 h were the strong carburizing period, with the carbon potential (Cp) of 1.0%, and the last 2 h were the diffusion period, with the Cp of 0.8%. After carburizing, the steel was sealed with anti-oxidation coating to avoid oxidation and decarburization during heat treatment. The process of secondary quenching after carburizing was austenitizing for 30 min at 900 °C. Then, the specimens were transferred quickly into salt baths with temperatures of 200 °C and 230 °C holding for different times, and, finally, tempered at 200 °C for 1 h.
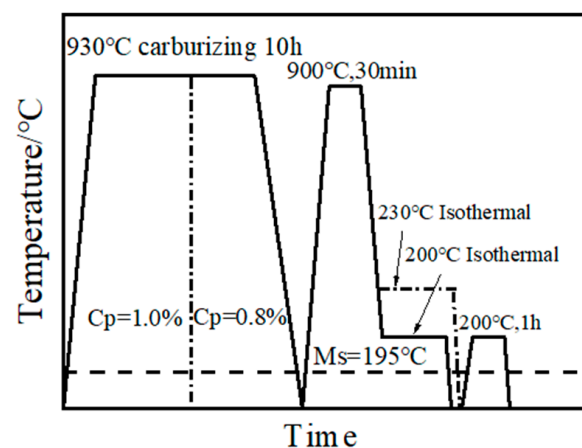

Figure 1. Schematic diagrams of carburizing and heat treatment processes.

After heat treatment, the anti-oxidation coating on the surface was removed. Then, the specimen surface was ground off 0.05 mm from the top surface using sandpaper and polished using polishing paste on a metallographic polishing machine. The microstructures of the experimental steel in different states were observed by OM (Axiovert200MAT, Carl Zeiss AG, Oberkochen, Germany), SEM (S-4800, Hitachi Limited, Tokyo, Japan), and TEM (JEM-2010, JEOL, Tokyo, Japan). The phase composition of the specimens was analyzed by XRD (D/MAX-2500/PC, Rigaku Corporation, Akishima, Japan).

The carbon content distribution of the carburizing layer was measured by a direct-reading spectrometer (PDA-5500II, Shimadzu, Kyoto, Japan). The hardness analysis required the dual analysis of surface hardness and cross-section hardness distribution. A digital Rockwell hardness tester (HRS-150, Laizhou Huayin Test Instrument Co., Ltd., Laizhou, China) was used to test the surface hardness of specimens. The hardness dis-

tributions of the carburized layer were tested on a Vickers hardness tester (FM-ARS9000, FUTURE-TECH, Tokyo, Japan), with an automatic micro-hardness testing system under the conditions of a load of 500 gf and a load retention time of 10 s. The tensile and impact tests were carried out on a MTS810 Landmark Servohydraulic Test System (MTS Systems, Eden Prairie, MN, USA) and NI300F impact test machine (NCS, Beijing, China), respectively. The friction and wear tests were carried out on a screen display end-face testing machine (MMU-5G, JiNan FangYuan testing machine, JiNan, China). The technical parameters selected for the wear test were as follows: the spindle speed was 200 r/min, and the load was 300 N. The total wear time of each specimen was 4 h. The quality change of the specimen was weighed by an electronic balance every 15 min during the wear process.

3. Experimental Results and Discussion

3.1. Microstructure

The optical micrographs of the carburized surface austempered at 200 °C and 230 °C for different times are shown in Figures 2 and 3, respectively. The black acicular areas in these figures are bainitic microstructure. Figure 2a shows that there is almost no bainitic ferrite generated in the microstructure, after austempering at 200 °C for 2 h. Figure 2b shows that there is a small amount of acicular bainitic ferrite appearing in the microstructure, after austempering at 200 °C for 4 h. After austempering at 230 °C for 2 h, there is a small amount of acicular bainitic ferrite appearing, which suggests that the incubation period at 230 °C is shorter than that at 200 °C. Furthermore, the bainitic ferrite content in the microstructure after isothermal treatment at 230 °C is higher than that after isothermal treatment at 200 °C, when the isothermal time is the same and the bainite transformation is not completed. Figures 2 and 3 show that the bainitic ferrite content, basically, increases with the increase in time. However, the bainitic ferrite content does not increase significantly, when the isothermal time extends from 24 h to 48 h at 230 °C. The bainite transformation is, basically, completed after isothermal treatment for 48 h at the two temperatures. Zhang et al. [10] reported that it needed 32 h to complete the bainite transformation at 220 °C on the surface for a carburized gear steel with the composition of Fe-0.81C-0.36Si-1.20Mn-1.35Cr-0.24Mo-0.92Al (wt.%).
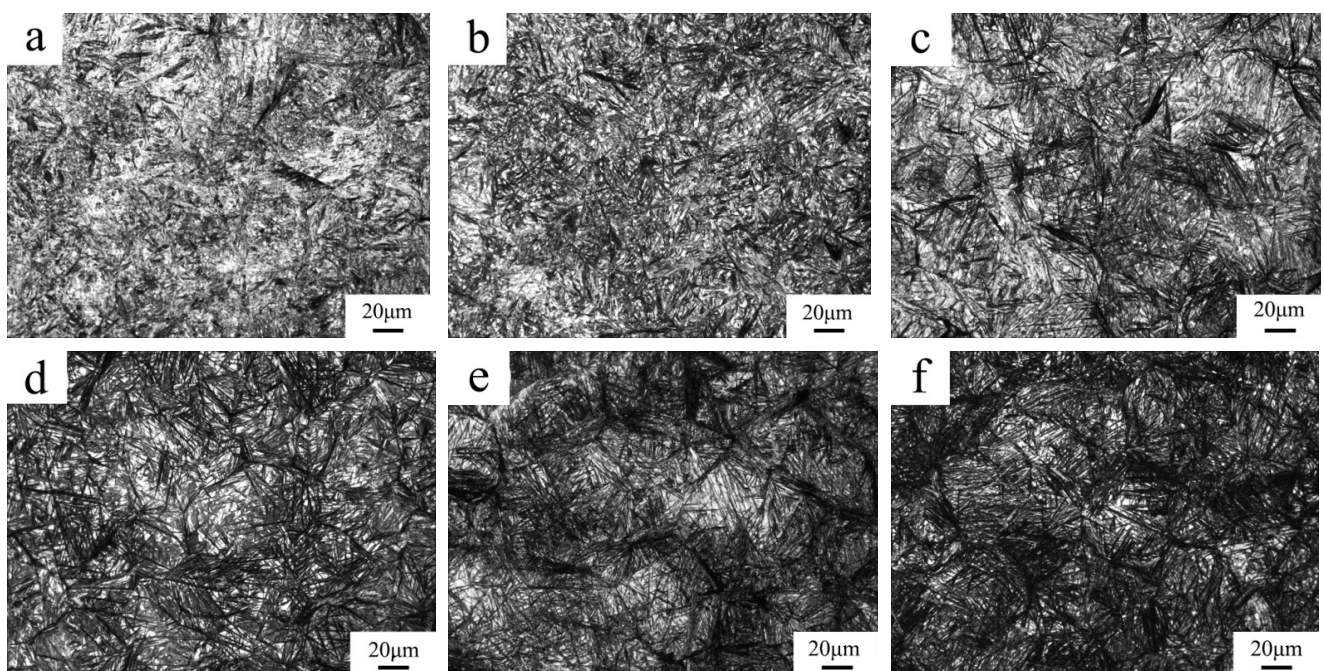

Figure 2. The optical micrographs of carburized surface austempered at 200 °C: (**a**) 2 h, (**b**) 4 h, (**c**) 8 h, (**d**) 12 h, (**e**) 24 h, and (**f**) 48 h.
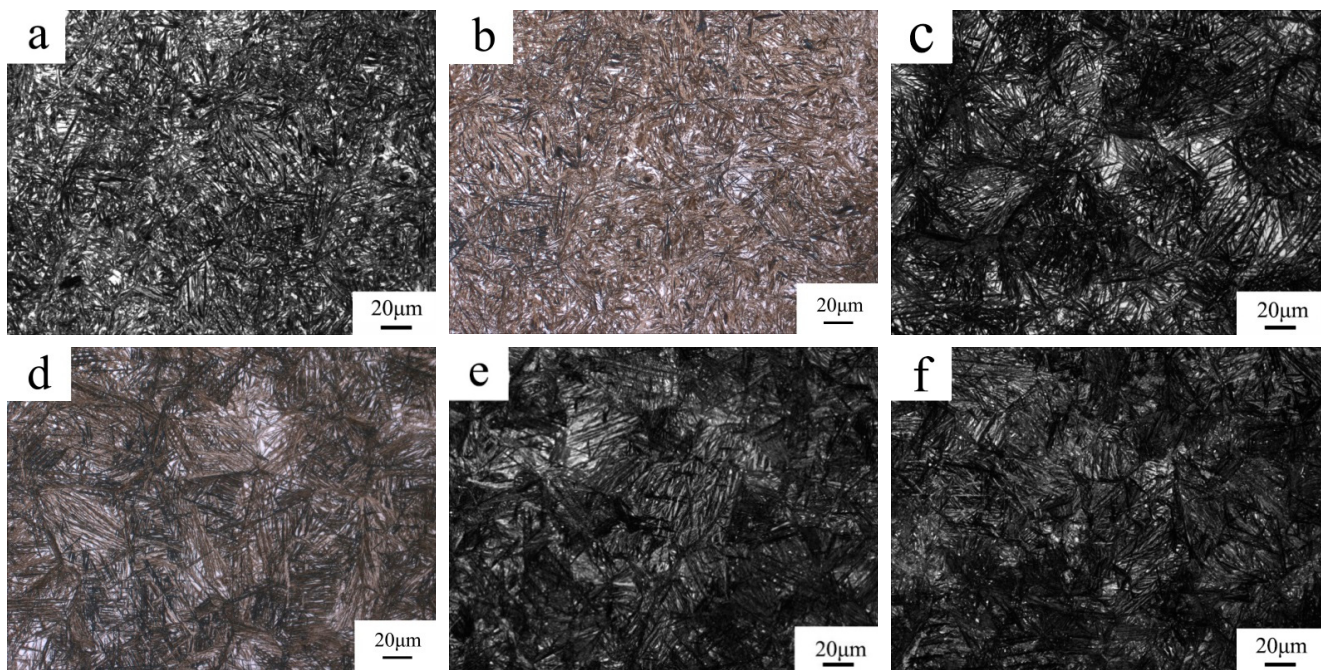
Figure 3. The optical micrographs of carburized surface austempered at 230 °C: (**a**) 2 h, (**b**) 4 h, (**c**) 8 h, (**d**) 12 h, (**e**) 24 h, and (**f**) 48 h.

The SEM images of the carburized surface austempered at 200 °C and 230 °C are shown in Figures 4 and 5, respectively. Figure 4a shows that the microstructure is mainly composed of martensite and retained austenite, and there is little bainitic ferrite formation on the carburized surface, after isothermal treatment at 200 °C for 2 h. The mixed microstructure composed of superfine bainitic ferrite, martensite, and retained austenite is obtained on the carburized surface, after holding at 200 °C for 8 h. Figure 5a shows that the microstructure of carburized surface is dominated by martensite and retained austenite, and there is only a small amount of bainitic ferrite formed after holding at 230 °C for 2 h. The dual-phase microstructure composed of superfine bainitic ferrite and retained austenite is observed on the carburized surface, after isothermal treatment at 200 °C and 230 °C for 48 h. There is no carbide found in the microstructure from SEM images. The superfine acicular bainitic ferrite microstructure is composed of many smaller sub lamellas, and the sub lamellas in the same bainitic lath are nearly parallel. Compared with martensite, the orientation of sub lamella in acicular bainitic ferrite microstructure is obvious.
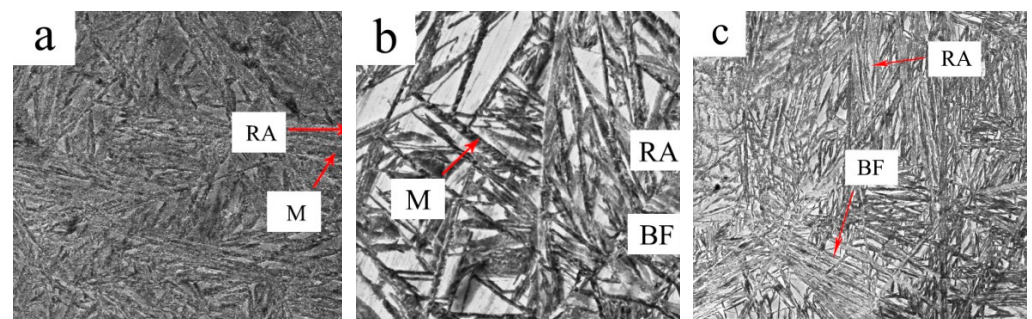

Figure 4. The SEM images of the carburized surface austempered at 200 °C: (**a**) 2 h, (**b**) 8 h, and (**c**) 48 h. Notes: BF—bainitic ferrite, RA—retained austenite, and M—martensite.

The TEM micrographs of the carburized surface, after isothermal treatment at 200 °C and 230 °C for 8 h and 48 h, are shown in Figure 6. In the figure, the bright area is bainitic ferrite lath, the dark area is retained austenite film, and the bainitic ferrite lath and retained

austenite film are basically arranged in parallel. In addition to bainitic ferrite and retained austenite, there is martensite on the carburized surface, after austempering at 200 °C for 8 h. There is only bainitic ferrite lath and retained austenite film, but no martensite, on the carburized surface after austempering for 48 h. A large number of TEM observations show that no carbides were observed in the bainitic ferrite lath, so the structure belongs to carbide-free bainitic ferrite. As for the complex addition of Si and Al, the solubility of Si and Al in carbide is very low [4,12], which can effectively inhibit the precipitation of carbide, resulting in no carbide formation in the microstructure.
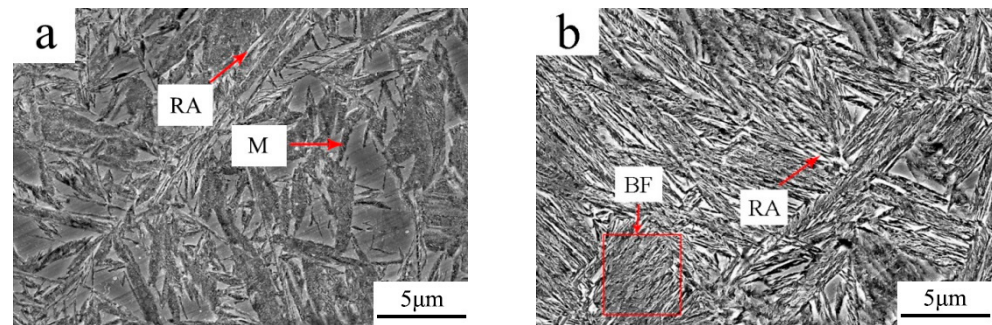

Figure 5. The SEM images of the carburized surface austempered at 230 °C: (**a**) 2 h and (**b**) 48 h. Notes: BF—bainitic ferrite, RA—retained austenite, and M—martensite.

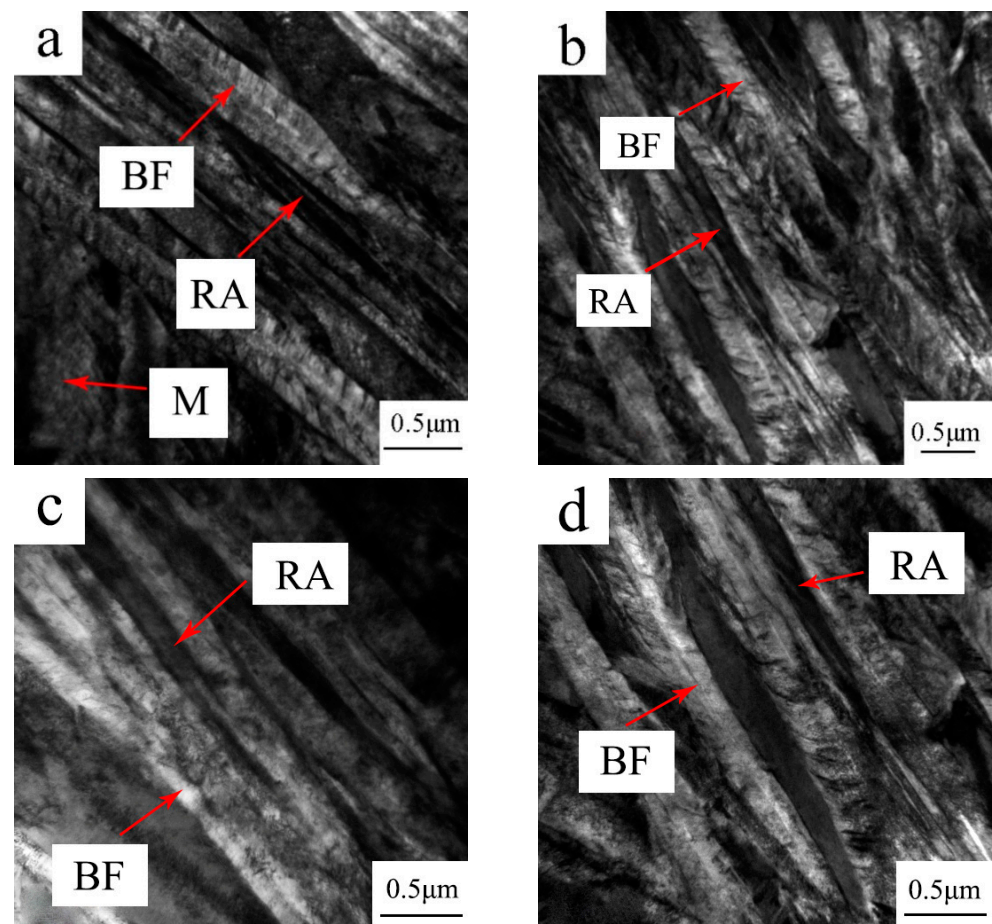**Figure 6.** The TEM micrographs of the carburized surface after isothermal treatment: (**a**) 200 °C × 8 h, (**b**) 200 °C × 48 h, (**c**) 230 °C × 8 h, and (**d**) 230 °C × 48 h. Notes: BF—bainitic ferrite, RA—retained austenite, and M—martensite.

According to the measurement and statistics results of the sizes of bainitic ferrite lath in a large number of TEM photos, the average thicknesses of bainitic ferrite lath on the carburized surface, after isothermal treatment at 200 °C and 230 °C for 8 h and 48 h, are 95 ± 11 nm, 90 ± 9 nm, 104 ± 10 nm, and 102 ± 9 nm, respectively. Zhang et al. [10] reported that the average thicknesses of bainitic ferrite lath in carburized gear steel, with the surface composition of Fe-0.81C-0.36Si-1.20Mn-1.35Cr-0.24Mo-0.92Al (wt.%), varied between 70 ± 7 nm and 160 ± 9 nm when it is austempered at 220 °C to 300 °C. The formation of superfine bainitic microstructure is mainly due to the low phase transformation temperature, the high C content of the surface after carburizing, and the high content (1.52 wt.%) of Si and Al in the steel. The high content of Si and Al prevents the precipitation of cementite during bainite transformation [4,11]. This superfine bainitic microstructure alleviates the stress concentration and relaxes the stress at the crack tip, so it hinders the initiation and propagation of cracks [8]. Thus, the superfine bainitic microstructure is beneficial to improve the wear resistance and fatigue properties of steel.

The XRD patterns of the carburized surface austempered at 200 °C and 230 °C are shown in Figure 7. It suggests that there are only ferrite (α) and austenite (γ) diffraction peaks on the carburized surface. The retained austenite content and carbon content in it were calculated using the empirical formula in Ref. [2], and the results are shown in Table 1. Obviously, the retained austenite content on the carburized surface, basically, shows a trend of gradual decline, with the increase in isothermal time from 8 h to 48 h at both temperatures. According to the XRD patterns (Figure 7), it is also obvious that the intensity of austenite diffraction peak decreases gradually with the increase in isothermal time. The retained austenite content calculated by XRD comes from two parts, one is the thin-film retained austenite in superfine bainitic microstructure, and the other is the block retained austenite between bainitic ferrite laths or martensite laths. The block retained austenite is metastable, and martensitic transformation can occur under stress, while the thin-film retained austenite is relatively stable [4]. The carbon-rich thin-film retained austenite is beneficial to improve the toughness and fatigue property, since it can reduce stress concentration and hinder the initiation and propagation of cracks.
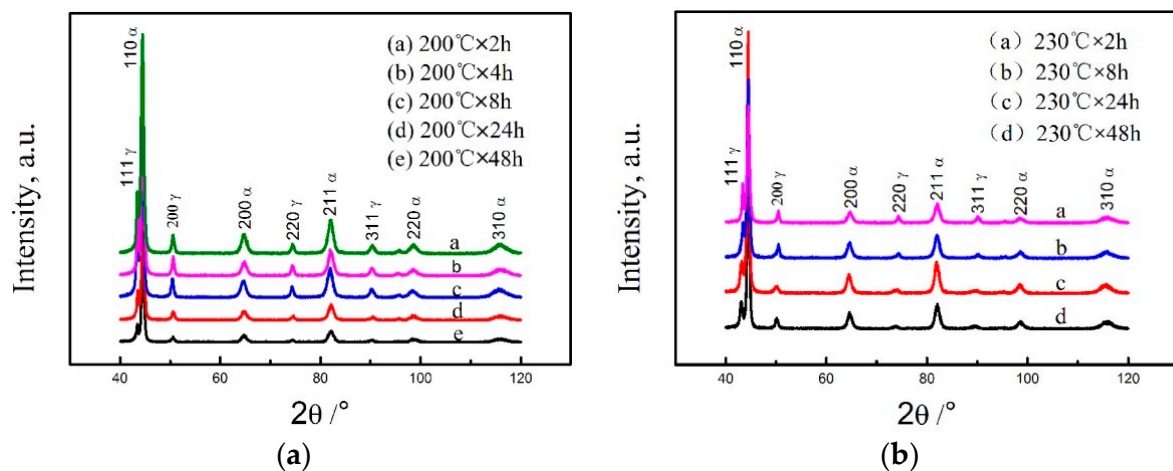

Figure 7. XRD patterns of carburized surface austempered at 200 °C (**a**) and 230 °C (**b**).

Table 1. Retained austenite content (V_γ), and the carbon content in it (C_γ), on carburized surface.

Isothermal Time		2 h	4 h	8 h	24 h	48 h
200 °C	V_γ (Vol.%)	23.3	30.1	27.0	20.7	15.6
	C_γ (wt.%)	0.93	0.99	0.90	0.87	0.85
230 °C	V_γ (Vol.%)	25.6	—	17.4	15.3	14.6
	C_γ (wt.%)	0.94	—	0.87	1.26	1.21

3.2. Distributions of Carbon Content and Hardness

The distribution curve of carbon content in the carburized layer is shown in Figure 8. One can see that the carbon content tends to decrease as the distance from the surface increases. The carbon content of the surface after carburizing is 0.82 wt.%, and the depth of the carburizing layer is about 2.5 mm, which meet the requirements of gear steel.
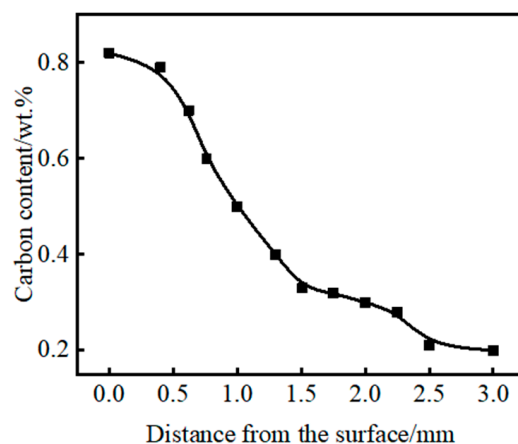

Figure 8. Carbon content distribution curve of the specimen after carburizing.

The Rockwell hardness values of the carburized surface austempered at 200 °C and 230 °C are shown in Table 2. With the increase in isothermal time, the hardness of carburized surface decreases gradually. With the extension of austempering time at 200 °C and 230 °C, more and more bainitic ferrite is formed in the microstructure. The microstructure dominated by martensite will gradually evolve into one dominated by bainitic ferrite, when the isothermal time is extended from 2 h to 48 h. The hardness of martensite is higher than that of bainite under the same composition [26,27]. Therefore, the hardness of carburizing surface decreases with the increase in holding time.

Table 2. Rockwell hardness of carburized surface (HRC).

Isothermal Time	2 h	4 h	8 h	12 h	24 h	48 h
200 °C	59.5 ± 0.3	59.0 ± 0.2	58.1 ± 0.3	57.8 ± 0.4	56.7 ± 0.1	56.9 ± 0.2
230 °C	58.0 ± 0.4	57.8 ± 0.3	56.4 ± 0.1	55.7 ± 0.3	55.7 ± 0.2	56.3 ± 0.3

The Vickers hardness distribution curves of the carburized layer austempered at 200 °C and 230 °C are shown in Figure 9. The hardness of the carburizing layer after austempering at 200 °C is higher than that at 230 °C, for the same time with the same distance from the surface, which is consistent with Table 2. The reasons for this phenomenon mainly come from two aspects. On one hand, the hardness value is closely related to the microstructure. The lower the transformation temperature is, the slower the transformation rate of bainitic ferrite is. Hence, the amount of bainitic ferrite of the specimen austempered at 200 °C is less than that of at 230 °C under the same time. On the other hand, as the austempering temperature decreases, the dislocation density increases and the bainitic ferrite becomes finer [30], which contribute greatly to the higher hardness.

When the holding time reaches 48 h, the surface hardness values of the specimens austempered at 200 °C and 230 °C are, basically, equivalent, which is about 610 HV. In addition, the hardness of the core is about 450 HV. The bainite transformation has, basically, been completed at 200 °C and 230 °C, while holding for 48 h, thus, the amounts of bainitic ferrite are almost the same. Besides, the contents of retained austenite on surfaces are close when the specimens are austempered at 200 °C and 230 °C for 48 h (see Table 1). Furthermore, the isothermal time of 48 h is long enough, so the diffusion of carbon atoms is sufficient. Therefore, the hardness values are similar.
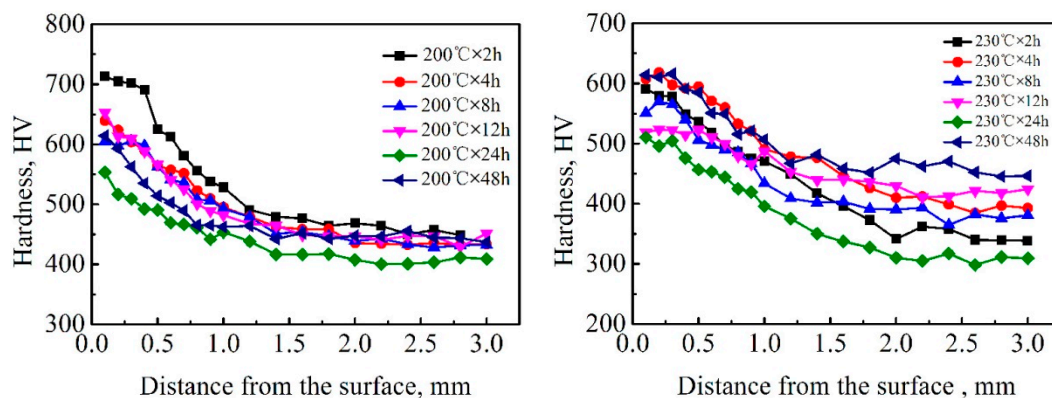
Figure 9. Vickers hardness distributions of carburized layer austempered at 200 °C (**left**) and 230 °C (**right**) for different times.

3.3. Wear Resistance

The relationship curves between weight loss and wear time of the carburized surface, after isothermal treatment at 200 °C, are shown in Figure 10. It is obvious that weight loss increases with the increase in wear time. The weight loss of carburized surface isothermal treated for 8 h is the least, while the weight loss of carburized surface isothermal treated for 48 h is the most. The hardness has a great influence on the wear resistance. The hardness values of carburized surfaces are 58.1 HRC and 56.7 HRC, after isothermal treatment for 8 h and 48 h, respectively, and the highest hardness is 59.5 HRC, after isothermal treatment for 2 h. The wear performance of carburized surface being isothermal treated for 2 h is better than that of being isothermal treated for 48 h. This is mainly because of the much higher hardness of a carburized surface being isothermal treated for 2 h than that of one isothermal treated for 48 h. The wear performance of a carburized surface after being isothermal treated for 8 h is better than that of a carburized surface with higher hardness, after being isothermal treated for 2 h. The microstructure of a carburized surface, after being isothermal treated for 2 h, is mainly martensite, while a large amount of bainitic ferrite is produced after being isothermal treated for 8 h. The study [4] has shown that the wear performance of bainite is higher than that of martensite with the same hardness. Therefore, the complexity of the wear mechanism suggests that the influencing factors of wear resistance are not only hardness but also many other factors such as microstructure, toughness, and so on. The result proves that the mixed microstructure of superfine bainitic ferrite and martensite has outstanding wear performance.
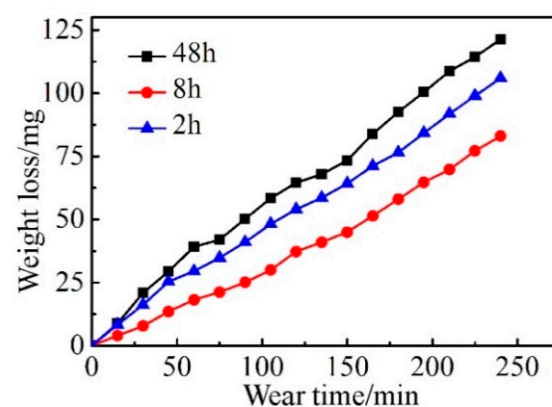

Figure 10. Relationship curves between weight loss and wear time of the carburized surface austempered at 200 °C.

A previous study of a Si-rich (1.43 wt.%) carburized bearing steel [26] has shown that the wear resistance of martensite/nano-bainite composite structure containing 47.2%

nano-bainite is better than that of the composite structures containing 23.8% and 62.9% nano-bainite, respectively. However, Zhao et al. [27] reported that the comprehensive mechanical properties and wear resistance of nano-bainite are better than those of the martensite or nano-bainite/martensite composite structures with different phase ratios in a Si/Al-rich bearing steel. The higher wear resistance is, mainly, due to the better thermal stability of the microstructure, after holding for longer time. Wang et al. [31] reported that aluminum can improve the wear resistance of bainitic steel, since aluminum promotes the formation of oxide film on wear surface and reduces the wear amount. However, when the content of aluminum is too high, the hardness of steel is reduced and the wear amount is increased.

The surface morphology images of the specimens after wear are shown in Figure 11. One can see that the carburized surfaces of the specimens, after isothermal treatment for 2 h and 8 h after wearing under 300 N for 4 h, are relatively smooth, with only small deformation bands found indicating high wear resistance, which might be related to the high hardness of the carburized surface. The worn surface of the specimen after isothermal treatment for 48 h is rough with furrows, a large area of spalling is found on the surface, and the small facet area caused by adhesion is large, which suggests poor wear resistance.
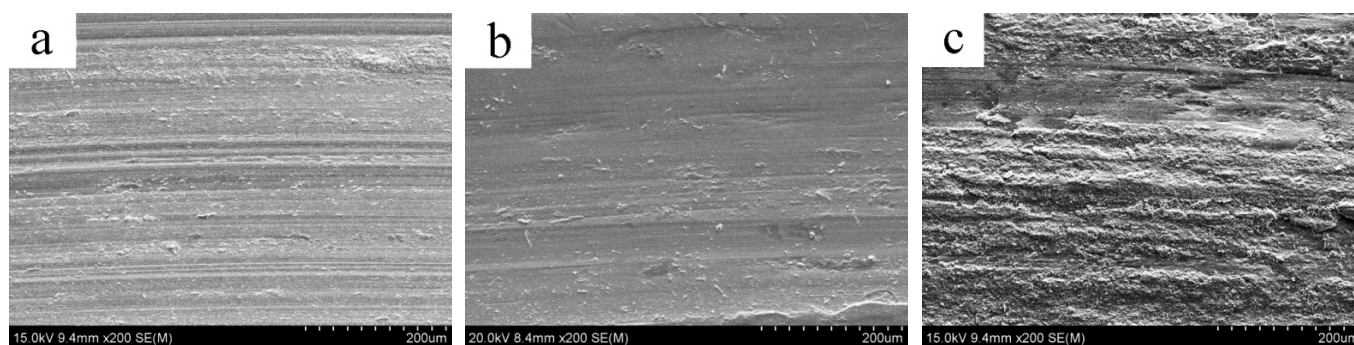

Figure 11. Wear morphology of carburized surface austempered at 200 °C: (**a**) 2 h, (**b**) 8 h, (**c**) 48 h.

The XRD patterns of the surface austempered at 200 °C for 8 h before and after wear testing are shown in Figure 12. The change of retained austenite content before and after wear is shown in Table 3. According to the data in Table 3 and the XRD patterns in Figure 12, the amount of retained austenite on the surface is considerably decreased after wear. During the wear process, shear stresses are produced on the friction surface, which causes dislocation slip in the steel, resulting in plastic deformation on the surface. The deformation results in the transformation of retained austenite to martensite, which reduces the amount of retained austenite and increases the amount of martensite. Although the surface hardness of the specimen isothermal treated for 2 h is higher, the ratio of retained austenite transformation on the surface of the specimen isothermal treated for 8 h before and after wear is about 1.6 times higher than that of the specimen isothermal treated for 2 h. The surface hardness increases, and the wear resistance is improved significantly, when a large amount of retained austenite transforms into martensite. Although the ratio of retained austenite transformation on the surface of the specimen isothermal treated for 48 h is also high, the improvement of wear resistance is limited, due to its low original surface hardness.

Table 3. The retained austenite content (Vol.%) of surface austempered at 200 °C before and after wear.

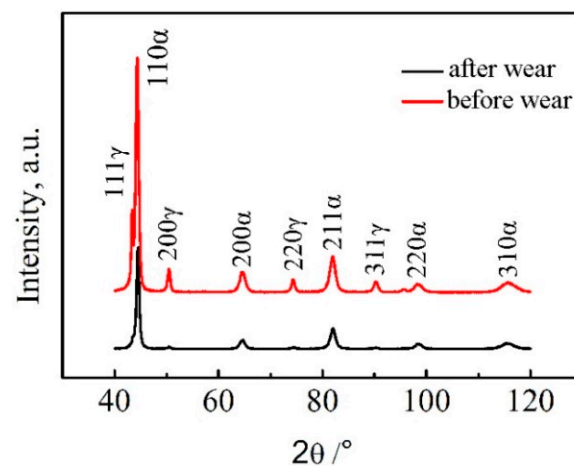| Isothermal Time	2 h	8 h	48 h
Before Wear	23.3	27.0	15.6
After Wear	12.8	8.0	4.9
Ratio of Transformation	45.1%	70.4%	68.6%

Figure 12. XRD patterns of the surface at 200 °C for 8 h before and after wear.

3.4. Microstructure and Mechanical Properties of the Core

As for gear steel, it not only requires high hardness and wear resistance of the surface but also high strength, good plasticity, and toughness of the core. The optical micrographs of the transition layer (1 mm away from the surface) and core of the experimental steel, after carburizing and austempering at 200 °C for 8 h, are shown in Figure 13. One can see that the microstructure of the transition layer consists of martensite, a small amount of bainitic ferrite, and retained austenite, while the core has a dual-phase microstructure consisting of much fine low-carbon lath martensite and retained austenite. The long-time holding at 200 °C has a certain tempering effect on the martensite generated during the austempering process in the core and transition layer, which plays a good role in reducing brittleness and improving the mechanical properties of quenched martensite.
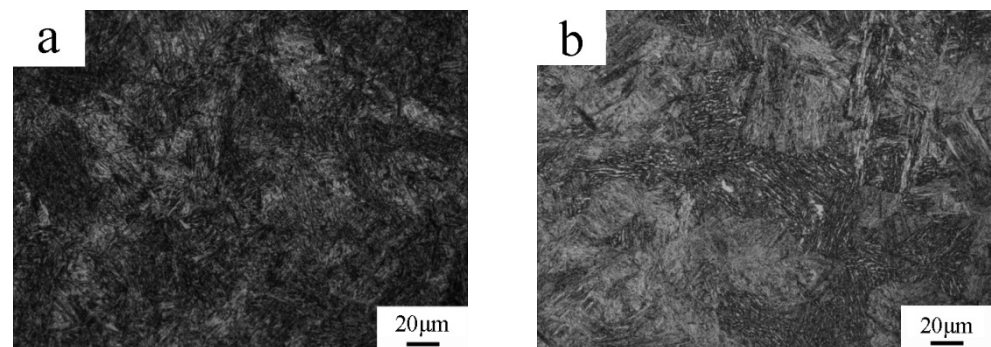

Figure 13. Optical micrographs of the transition layer (**a**) and core (**b**) of the experimental steel, after carburizing and austempering at 200 °C for 8 h.

Heavy-duty gear steel requires not only high surface hardness, but also high strength and toughness in the core. The specific technical requirements are as follows: core hardness is 30~45 HRC, tensile strength is 1100~1200 MPa, impact energy is greater than 100 J, tooth surface hardness is 58~62 HRC, and the amount of retained austenite is less than or equal to 30 vol.%. Table 4 shows the mechanical properties in the core of the experimental steel, after carburizing and austempering at 200 °C for 8 h. According to the data in the table, the tensile strength is 1217 MPa and the impact energy is 156 J. The strength and toughness are well matched. Besides, the surface hardness is 58.1 HRC, and the amount of retained austenite on the surface is 27 vol.%, under the same process as the core. Therefore, the experimental steel can fully meet the requirements for the mechanical properties of heavy-duty gear.

Table 4. Mechanical properties in the core, after carburizing and austempering at 200 °C for 8 h.

Hardness	Impact Energy	Yield Strength	Tensile Strength	Elongation	Reduction of Area
34.4 HRC	156 J	731 MPa	1217 MPa	11.6%	40.3%

The excellent combination of strength and toughness of the core is, firstly, due to the much fine low-carbon lath martensite obtained in the core during isothermal quenching. Ref. [26] has also shown that the martensite formed by isothermal quenching is finer than that of oil quenching. Secondly, the 200 °C isothermal process can eliminate the stresses caused by quenching and martensitic transformation, and the higher quenching temperature greatly reduces the number of microcracks caused by quenching stress, which play an important role in improving strength and toughness of the steel. Furthermore, due to the addition of the non-carbide-forming element Si, which has a pinning effect on dislocations, the strength and toughness are improved significantly.

4. Conclusions

Several conclusions are drawn below.

1. In this paper, the designed low-carbon Si/Al-rich alloy steel was carburized and austempered at a temperature slightly higher than the Ms point of the carburized surface. The mixed microstructure, consisting of superfine bainitic ferrite with thickness around 100 nm and martensite, was obtained on the surface, and the fine low-carbon lath martensite was obtained in the core.

2. The mixed microstructure of superfine bainitic ferrite and martensite was obtained on the carburized surface, austempered at 200 °C for 8 h, and its wear resistance was not only higher than that of the surface isothermal treated for 2 h, with martensite as the main phase, but also higher than that of the surface isothermal treated for 48 h, with superfine bainitic ferrite as the main phase. Its excellent wear resistance is due to the high hardness of its mixed microstructure and the higher amount of retained austenite transformation during the wear process.

3. After carburizing and austempering at 200 °C for 8 h, the hardness and the amount of retained austenite on the surface of the experimental steel are 58.1 HRC and 27 vol.%, respectively, while the hardness, tensile strength, and impact energy of the core are 34.4 HRC, 1217 MPa, and 156 J, respectively. Therefore, the experimental steel fully meets the requirements for the mechanical properties of heavy-duty gear and is expected to be utilized in the manufacture of heavy-duty gear.

Author Contributions: Conceptualization, Y.W. and Q.H.; formal analysis, Q.Y., D.X. and F.Z.; investigation, Z.Y. and F.Z.; methodology, Q.H. and Q.Y.; project administration, Y.W., D.X. and Z.Y.; writing—original draft, Y.W., Q.H. and Z.Y.; writing—review & editing, F.Z. All authors have read and agreed to the published version of the manuscript.

Data Availability Statement: The data presented in this study are available on request from the corresponding author.

Conflicts of Interest: The authors declare no conflict of interest.

References

1. Zhang, F.; Huang, Z.Z.; Zhao, S.X.; Gao, J.Q.; Zhang, X.Z.; Zhang, J.; Wang, W. Carbide-Free Bainite Steel for Electric Vehicle Gear and a Production Method Thereof. Chinese Invention Patent. CN 111471938 A, 2020.
2. He, Q.S. *Application of Carburized Bainite Steel in Bearing and Gear*; Yanshan University: Qinhuangdao, China, 2014.
3. Bhadeshia, H.K.D.H. Nanostructured bainite. *Proc. R. Soc. A* **2010**, *466*, 3–18. [CrossRef]
4. Bhadeshia, H.K.D.H. *Bainite in Steels*, 3rd ed.; Maney Publishing: Leeds, UK, 2015.
5. Liu, M.; Fan, Y.S.; Gui, X.L.; Hu, J.; Wang, X.; Gao, G.H. Relationship between Microstructure and Properties of 1380 MPa Grade Bainitic Rail Steel Treated by Online Bainite-Based Quenching and Partitioning Concept. *Metals* **2022**, *12*, 330. [CrossRef]
6. Zhao, J.L.; Lv, B.; Zhang, F.C.; Yang, Z.N.; Qian, L.H.; Chen, C.; Long, X.X. Effects of austempering temperature on bainitic microstructure and mechanical properties of a high-C high-Si steel. *Mater. Sci. Eng. A* **2019**, *742*, 179–189. [CrossRef]
7. Krolicka, A.; Radwanski, K.; Ambroziak, A.; Zak, A. Analysis of grain growth and morphology of bainite in medium-carbon spring steel. *Mater. Sci. Eng. A* **2019**, *768*, 138446. [CrossRef]
8. Wang, Y.H.; Yang, Z.N.; Zhang, F.C.; Qin, Y.M.; Wang, X.B.; Lv, B. Microstructures and properties of a novel carburizing nanobainitic bearing steel. *Mater. Sci. Eng. A* **2020**, *777*, 139086. [CrossRef]
9. Yue, X.; Hu, S.; Wang, X.K.; Liu, Y.X.; Yin, F.; Hua, L. Understanding the nanostructure evolution and the mechanical strengthening of the M50 bearing steel during ultrasonic shot peening. *Mater. Sci. Eng. A* **2022**, *836*, 142721. [CrossRef]
10. Zhang, P.; Zhang, F.C.; Wang, T.S. Preparation and microstructure characteristics of low-temperature bainite in surface layer of low carbon gear steel. *Appl. Surf. Sci.* **2011**, *257*, 7609–7614. [CrossRef]
11. Yang, J.; Wang, T.S.; Zhang, B.; Zhang, F.C. Microstructure and mechanical properties of high-carbon Si–Al-rich steel by low-temperature austempering. *Mater. Des.* **2012**, *35*, 170–174. [CrossRef]
12. Garcia-Mateo, C.; Caballero, F.G.; Bhadehia, H.K.D.H. Acceleration of Low-temperature Bainite. *ISIJ Int.* **2003**, *43*, 1821–1825. [CrossRef]
13. Hu, F.; Wu, K.M.; Zheng, H. Influence of Co and Al on bainitic transformation in super bainitic steels. *Steel Res. Int.* **2013**, *84*, 1060–1065. [CrossRef]
14. Huang, H.; Sherif, M.Y.; Rivera-Díaz-del-Castillo, P.E.J. Combinatorial optimization of carbide-free bainitic nanostructures. *Acta Mater.* **2013**, *61*, 1639–1647. [CrossRef]
15. Gong, W.; Tomota, Y.; Adachi, Y. Effects of ausforming temperature on bainite transformation, microstructure and variant selection in nanobainite steel. *Acta Mater.* **2013**, *61*, 4142–4154. [CrossRef]
16. Golchin, S.; Avishan, B.; Yazdani, S. Effect of 10% ausforming on impact toughness of nano bainite austempered at 300 °C. *Mater. Sci. Eng. A* **2016**, *656*, 94–101. [CrossRef]
17. He, J.G.; Zhao, A.M.; Zhi, C.; Fan, H.L. Acceleration of nanobainite transformation by multi-step ausforming process. *Scr. Mater.* **2015**, *107*, 71–74. [CrossRef]
18. Hu, H.J.; Hatem, S.Z.; Xu, G.; Embury, D. New insights to the effects of ausforming on the bainitic transformation. *Mater. Sci. Eng. A* **2015**, *626*, 34–40. [CrossRef]
19. Zhao, J.; Wang, Y.F.; Guo, K.; Wang, Y.H.; Jia, N. Transformation behavior and microstructure feature of large strain ausformed low-temperature bainite in a medium C-Si rich alloy steel. *Mater. Sci. Eng. A* **2017**, *682*, 527–534. [CrossRef]
20. Toji, Y.; Matsuda, H.; Raabe, D. Effect of Si on the acceleration of bainite transformation by pre-existing martensite. *Acta Mater.* **2016**, *116*, 250–262. [CrossRef]
21. Zhao, L.J.; Qian, L.H.; Meng, J.Y.; Zhou, Q.; Zhang, F.C. Below-Ms austempering to obtain refined bainitic structure and enhanced mechanical properties in low-C high-Si/Al steels. *Scr. Mater.* **2016**, *112*, 96–100. [CrossRef]
22. Santigopal, S.; Pinaki, B.; Sushil, G.; Shiv, B.S.; Saurabh, K. Formation of bainite below the Ms temperature: Kinetics and crystallography. *Acta Mater.* **2016**, *105*, 390–403.
23. Santigopal, S.; Pinaki, B.; Shiv, B.S. Analysis of the kinetics of bainite formation below the Ms temperature. *Scr. Mater.* **2017**, *136*, 132–135.
24. Tian, J.Y.; Xu, G.; Zhou, M.X.; Hu, H.J. Refined Bainite Microstructure and Mechanical Properties of a High-Strength Low-Carbon Bainitic Steel Treated by Austempering below and above Ms. *Steel Res. Int.* **2018**, *89*, 1700469. [CrossRef]
25. Liu, H.J.; Sun, J.J.; Jiang, T.; Guo, S.W.; Liu, Y.N. Improved rolling contact fatigue life for an ultrahigh-carbon steel with nanobainitic microstructure. *Scr. Mater.* **2014**, *90–91*, 17–20. [CrossRef]
26. Wang, Y.H.; Yang, Z.N.; Zhang, F.C.; Wu, D.D. Microstructures and mechanical properties of surface and center of carburizing 23Cr2Ni2Si1Mo steel subjected to low-temperature austempering. *Mater. Sci. Eng. A* **2016**, *670*, 166–177. [CrossRef]
27. Zhao, J.; Wang, T.S.; Lv, B.; Zhang, F.C. Microstructures and mechanical properties of a modified high-C–Cr bearing steel with nano-scaled bainite. *Mater. Sci. Eng. A* **2015**, *628*, 327–331. [CrossRef]
28. Gong, W.; Tomota, Y.; Harjo, S.; Su, Y.H.; Aizawa, K. Effect of prior martensite on bainite transformation in nanobainite steel. *Acta Mater.* **2015**, *85*, 243–249. [CrossRef]
29. Gao, G.H.; An, B.F.; Zhang, H.; Guo, H.R.; Gui, X.L.; Bai, B.Z. Concurrent enhancement of ductility and toughness in an ultrahigh strength lean alloy steel treated by bainite-based quenching-partitioning-tempering process. *Mater. Sci. Eng. A* **2017**, *702*, 104–112. [CrossRef]

30. Wang, Y.H.; Zhang, F.C.; Wang, T.S. A novel bainitic steel comparable to maraging steel in mechanical properties. *Scr. Mater.* **2013**, *68*, 763–766. [CrossRef]

31. Wang, M.M.; Lv, B.; Yang, Z.N.; Zhang, F.C. Wear resistance of bainite steels that contain aluminium. *Mater. Sci. Technol.* **2016**, *32*, 282–290. [CrossRef]